Mat. Res. Soc. Symp. Proc. Vol. 661 © 2001 Materials Research Society

Electrospinning of Polymeric Nanofibers: Analysis of Jet Formation

Antonio E. Senador Jr.[b], Montgomery T. Shaw[a,b], and Patrick T. Mather[a,b,*]
[a]Polymer Program, Institute of Material Science, and [b]Chemical Engineering,
University of Connecticut, Storrs, CT 06269, U.S.A.

ABSTRACT

Producing nanofiber-diameter polymeric fibers presents an attractive and robust approach toward the processing of nanocomposites, with applications ranging from clear optical components to toughened structural materials. In this work, we are examining the electrospinning process for the production of nanometer-diameter polymer fibers, giving particular attention to the following key features: jet-initiation, fiber architecture, and fiber distribution. A wide range of polymer systems and polymer-solvent combinations were studied in order to broaden the applicability of our conclusions to other systems. Specifically, a dimensional analysis was applied to jet-formation data obtained by quantifying the conditions required for the expulsion of fibers from a charged capillary to a grounded collection plate. The relationships between various dimensionless groups were compared with the expressions for the critical voltage that have been proposed for electrospinning of polymer solutions.

INTRODUCTION

The use of high voltage, alone or in combination with mechanical means, to spin fibers from solutions and melts have been around for at least 75 years now [1,2], but research became rejuvenated in mid-1990's [3] due to increasing interests in nanomaterials. Prior to this, the electrospinning process has been known to consistently produce fibers in the order of 1 μm, with some excursions into the upper nanometer range. At this early stage, it was already noted that the jet-formation mechanism plays a significant part in the control of the fiber diameter, leading to the establishment of some semi-empirical relationships [1,4].

Apart from finding unique applications for electrospun nanofibers, current research effort is also being focused on improving the process model. An example of this is the modeling of the jet as it extends under the influence of the external field and the repulsion between charge carriers [5,6,7]. However, overly simplistic rules for the initiation of the jet from a Taylor-cone meniscus are still being employed. For example, they often exclude such fluid properties as viscosity and conductivity – properties that vary significantly between polymer melts and solutions, for example. In this work, we quantify the effect of solution properties on the formation of the liquid jet.

EXPERIMENTAL DETAILS

The polymer-solvent systems used are listed in Table 1, where it can be seen that we have varied the polymer, solvent, and solution concentration systematically to vary such physical properties as electrical conductivity, viscosity, and surface tension over large ranges. While electrospinning from aqueous solutions of poly(ethylene oxide) (PEO) and poly(vinyl alcohol) (PVA) have already been reported [8,9], there is no previous study reporting the production of

polystyrene (PS) fibers. The selection of the polystyrene-chloroform system was mostly arbitrary, although the ease of preparing the solution and the volatility of the solvent were taken into consideration. As for the polystyrene- (tetrahydrofuran/ N,N-dimethylformamide) solution, the solvent mixture has been used previously to optimize the volatility during the electrospinning of poly(styrene-*block*-butadiene-*block*-styrene) [10].

Table 1. Solution properties and process parameters used.

Polymer-solvent System	Density ρ, g/mL	Viscosity η, Pa s	Surface Tension σ, dyne/cm	Voltage **E**, kV	Needle-Collector Gap **h**, cm	Resistivity $1/\sigma_e$, Ω cm	Dielectric Constant ε_r
4%PEO-(20%H_2O/80%Ethanol)	0.8676	0.025	25.3	9	5	2.32E+05	32.9
6%PEO-(20%H_2O/80%Ethanol)	0.8589	0.036	25.7	9	5	1.44E+05	32.4
8%PEO-(20%H_2O/80%Ethanol)	0.8584	0.07	26.1	9	5	2.27E+05	31.9
10%PEO-(20%H_2O/80%Ethanol)	0.8527	0.183	26.5	9	5	2.29E+05	31.5
2.5%PS-$CHCl_3$	1.4836	0.002	25.5	9	10	7.09E+08	4.76
5%PS-$CHCl_3$	1.4752	0.004	25.9	9	10	9.44E+08	4.71
7.5%PS-$CHCl_3$	1.4667	0.008	26.6	9	10	6.66E+08	4.67
10%PS-$CHCl_3$	1.4583	0.014	26.4	9	10	7.46E+08	4.62
7%PS-(75%THF/25%DMF)	0.9129	0.011	25.9	9	6	7.29E+06	14
7%PS-(50%THF/50%DMF)	0.9256	0.012	28.5	9	6	3.15E+06	21
7%PS-(25%THF/75%DMF)	0.9387	0.011	31.8	9	6	3.02E+06	28.1
4%PVA-H_2O	1.0099	0.023	45.2	9	3	1.37E+04	75.7
6%PVA-H_2O	1.0158	0.09	49.5	10	3.3	8.90E+03	74.6
8%PVA-H_2O	1.0202	0.291	55.5	10	3.3	1.51E+04	73.4
10%PVA-H_2O	1.025	0.846	60.2	10	3.3	8.90E+03	72.2

Note: The needle radius used was **r** = 0.25 mm in all runs.

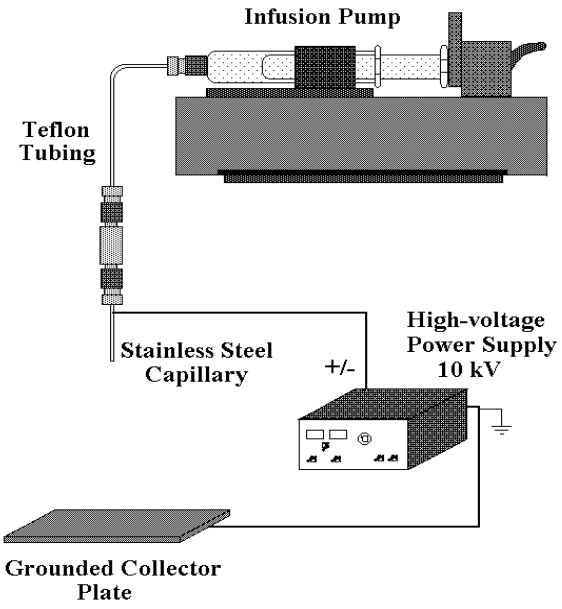

Figure 1. Schematic of the electrospinning setup used.

The solution properties of these systems were measured with CAHN dynamic contact angle analyzer (surface tension), Paar Physica controlled-stress rheometer fitted with concentric-cylinder fixture (viscosity), and an improvised conductivity meter (electrical resistance). These properties span a wide range, which makes dimensionless analysis suitable from the jet-initiation data.

A schematic of the experimental set-up used is shown in Figure 1. It consists of a Harvard Apparatus infusion pump fitted with a 5-cc glass syringe. Teflon™ and Kel-F™ tubing and fittings transport the polymer solution from the syringe to the mounted needle. A circular plate wrapped with aluminum foil served as the grounded collector. The needle was placed at high positive voltage using a Gamma High Voltage power supply. The current carried by the material being collected was monitored by measuring the voltage across a 1-kΩ shunt resistor placed between the collector and the ground terminal of the power supply.

DISCUSSION

Listed in Table 2 are the process variables and material properties that have been thought to influence the jet near the capillary [1,4,8]. From these quantities, a dimensionless relationship can be conceived by selecting an arbitrary subset from the list to be used as primary variables to then treat the rest as derived variables. However, consideration of electrical quantities had been known to complicate this approach since these could be included in a number of dimensionless groups [11]. Thus, to make the adopted electrical system obvious, all selected variables were expressed in terms of the independent reference quantities of length, time, mass, and charge.

These ten parameters and four reference quantities yielded 164 feasible sets of six dimensionless groups out of 210 possible combinations. The set used in the subsequent analysis was

$$F\left\{\left(\frac{\eta}{\sqrt{\rho r \sigma}}\right),\left(E\sqrt{\frac{\varepsilon_e}{r\sigma}}\right),\left(\frac{\sigma_e}{\varepsilon_e}\sqrt{\frac{\rho r^3}{\sigma}}\right),\left(\frac{h}{r}\right),\left(\frac{I r^2}{\sigma}\sqrt{\frac{\rho}{\varepsilon_e}}\right),\left(q\sqrt{\frac{\rho}{r^3\sigma}}\right)\right\}=1, \qquad (1)$$

where $F(\cdot)$ is an undetermined function relating the dimensionless groups. This set was selected because of the convenience it presents in interpreting each term. From left to right, the groups represent viscosity, voltage, conductivity, capillary-to-collector distance, current density, and volumetric flow rate. The other variables serve to normalize the data with a reference force (surface tension) and a geometric parameter (capillary radius), or to provide conversion between mechanical and electrical variables (dielectric permittivity).

In gathering data for the analysis of the jet formation phenomena, the process variables were adjusted until a deformed convex meniscus appeared at the tip of the capillary. Then, the applied voltage was increased until a jet was ejected from the meniscus, and the values of the process variables noted at this point. Current and flow rate are not factors at the threshold of jet formation, so the last two dimensionless groups in the chosen set can be neglected. Thus a general relationship between the critical voltage and other variables during jet formation can be written as,

$$E\sqrt{\frac{\varepsilon_e}{r\sigma}} = F\left\{\left(\frac{\eta}{\sqrt{\rho r \sigma}}\right),\left(\frac{\sigma_e}{\varepsilon_e}\sqrt{\frac{\rho r^3}{\sigma}}\right),\left(\frac{h}{r}\right)\right\}. \qquad (2)$$

For comparison, a survey of the literature yields a number of semi-empirical equations for the critical voltage; a summary is given in Table 3. Such expressions were intended to estimate the critical voltage requirement (E) in electrostatic spraying of liquids, and were used in electrospinning by previous investigators because of similarity between the two processes. We have recast these equations into forms allowing direct comparison with equation (2). All constants were lumped as C_1, and the natural logarithm function in the first equation was represented as F_1. The variable L in the first equation is the length of the capillary, which was not included in our dimensionless analysis.

Table 2. Listing of the variables used in dimensional analysis.

Variable	Symbol	Dimensions
Density	ρ	$M\,L^{-3}$
Capillary radius	r	L
Viscosity	η	$M\,L^{-1}\,T^{-1}$
Surface tension	σ	$M\,T^{-2}$
Voltage	E	$M\,L^{2}\,T^{-2}\,Q^{-1}$
Conductivity	σ_e	$M^{-1}\,L^{-3}\,T\,Q^{2}$
Capillary-to-collector gap	h	L
Dielectric permittivity	$\varepsilon_e \equiv \varepsilon_r \varepsilon_0$	$M^{-1}\,L^{-3}\,T^{2}\,Q^{2}$
Current density (current/area)	I	$L^{-2}\,T^{-1}\,Q$
Volumetric flow rate	q	$L^{3}\,T^{-1}$

Reference quantities: M (mass), L (length), T (time), and Q (charge) [14]

Table 3. Known expressions for the critical voltage.

Original equations	Recast equations	References
$E^2 = 4\left(\frac{h}{L}\right)^2\left(\ln\frac{2L}{r}-1.5\right)(0.117\pi r\sigma)$	$E\sqrt{\frac{\varepsilon_e}{r\sigma}} = C_1\left(\frac{h}{L}\right)F_1\left(\frac{L}{r}\right)$	4
$E = 300\sqrt{20\pi\sigma r}$	$E\sqrt{\frac{\varepsilon_e}{r\sigma}} = C_1$	1
$E = 0.863\sqrt{\frac{\sigma h}{\varepsilon_0}}$	$E\sqrt{\frac{\varepsilon_e}{r\sigma}} = C_1\left(\frac{h}{r}\right)^{1/2}$	12
$\frac{E}{h} = \sqrt{\frac{4\sigma}{\varepsilon_0 r}}$	$E\sqrt{\frac{\varepsilon_e}{r\sigma}} = C_1\left(\frac{h}{r}\right)$	13

Inspection of the recast equations of Table 3 reveals that they predict the dimensionless critical voltage, $E/h\sqrt{\varepsilon_e r/\sigma}$, to be either constant or a function only of the geometric ratio (h/r) with a power-law exponent of 0.5 or 1. None of the equations includes the possible dependence of the critical voltage on viscosity or conductivity as represented by the other two dimensionless groups, although the investigators themselves mentioned their possible importance.

To check this, the dependence on the geometric group was assumed to be 1st power, allowing simplification of the dimensionless relationship of equation (2) to,

$$\frac{E}{h}\sqrt{\frac{\varepsilon_e r}{\sigma}} = F\left\{\left(\frac{\eta}{\sqrt{\rho r\sigma}}\right),\left(\frac{\sigma_e}{\varepsilon_e}\sqrt{\frac{\rho r^3}{\sigma}}\right)\right\}. \qquad (3)$$

We note that the first term in $F(\cdot)$ is equivalent to the Ohnesorge number (*Oh*) – viscous force to surface force – while the second term is a dimensionless electrical conductivity or the ratio of Raleigh time to charge relaxation time.

Values for each group in equation (3) were calculated using critical voltage data obtained from the electrospinning of the solutions listed in Table 1, and the results are graphed in Figures 2 and 3. The first graph indicates a strong dependence on *Oh* between material systems, along with a consistent negative slope within each system. The second graph, on the other hand, shows a 0.25 power-law dependence of the critical voltage on the electrical conductivity of the solution. This weak dependence may have gone unnoticed previously, since typical studies have been restricted to one or two polymer-solvent systems at a time, the differences in electrical conductivity being small. Consideration of both Figure 2 and Figure 3 clearly reveals the relevance of both dimensionless groups.

In contrast, the equation for the critical voltage from reference [13], for example, implies that the data points in Figures 2 and 3 should lie on a single horizontal line. Although this is roughly the case within a polymer-solvent system, it cannot account for the variation between systems. Furthermore, the equation predicts that a log-log plot of E/h against (σ/r) would yield a line with a slope of 0.5. Figure 4 shows that, while the plot is virtually horizontal within each system, it does reveal slope significantly larger than 0.5 (line shown) predicted from reference [13]. However, our experimental data must be greatly expanded to test this finding rigorously.

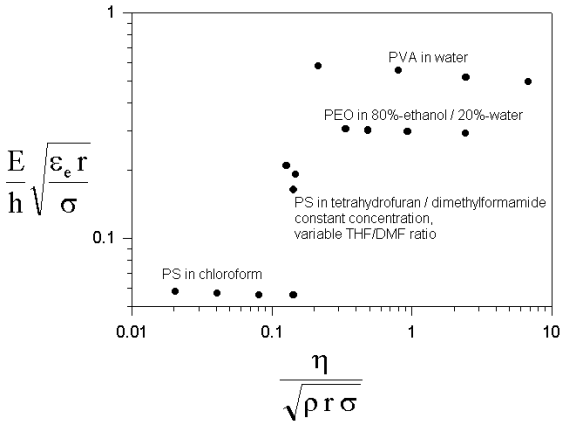

Figure 2. Plot of the dimensionless critical voltage versus the dimensionless viscosity.

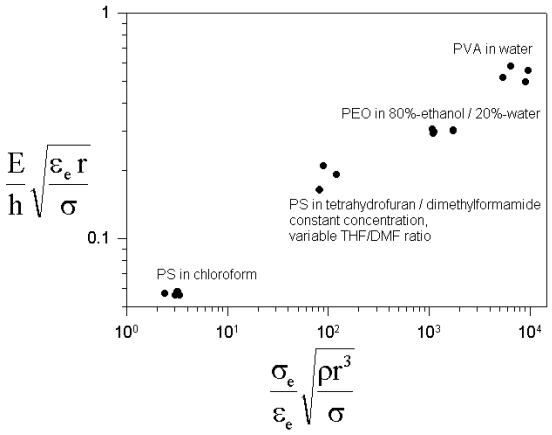

Figure 3. Plot of the dimensionless critical voltage versus dimensionless conductivity.

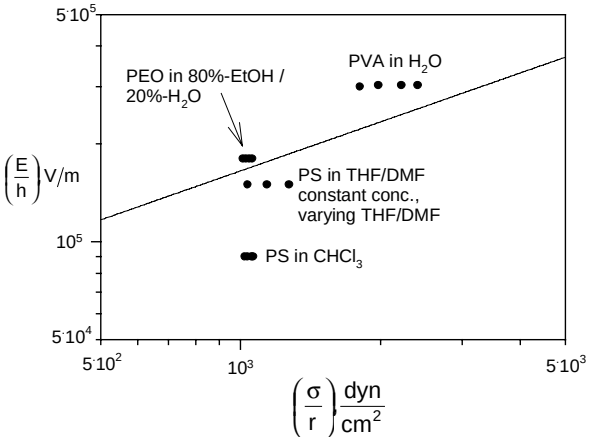

Figure 4. Plot of the critical voltage, following reference [13].

CONCLUSIONS

A general relationship between process parameters and solution properties was

derived using dimensionless analysis to describe the critical voltage requirement for initiating the liquid jet in electrospinning. Plots of the data from polymer solutions with very different properties indicate that the viscosity, surface tension, conductivity, and dielectric constant of the fluid could simultaneously affect the voltage required for jet-formation. The semi-empirical equations suggested before must be revised to include them. We note that our experimental data is preliminary in nature and present studies are focusing on expanding the breadth of solution physical properties and the conditions under which jet formation is examined.

ACKNOWLEDGEMENTS

This work is supported in part by grants from the University of Connecticut Research Foundation (PTM) and Connecticut Innovations, Inc. (PTM and MTS). Ms. N. LeBouch is acknowledged for help with surface tension and electrical resistance measurements.

REFERENCES

1. P. K. Baumgarten, *J. Colloid Interface Sci*. **36**, 71 (1971).
2. A. G. Bailey, *Electrostatic Spraying of Liquids*, (Research Studies Press, England, 1988).
3. D. H. Reneker, I. Chun, *Nanotechnology* **7**, 216 (1996).
4. L. Larrondo, R. St. John Manley, *J. Polym. Sci.: Polym. Phys.* **19**, 909 (1981).
5. D. H. Reneker, et. al, *J. Appl. Phys*. **87** (9), 4531 (2000).
6. A. F. Spivak, Y. A. Dzenis, D. H. Reneker, *Mech. Res. Comm*. **27** (1), 37 (2000).
7. M. A. Johnson, D. C. Martin, presented at the 1998 MRS Fall Meeting (unpublished).
8. H. Fong, I. Chun, D. H. Reneker, *Polymer* **40**, 4585 (1999).
9. R. Jaeger, et. al., *Macromol. Symp.* **127**, 141 (1998).
10. H. Fong, D. H. Reneker, *J. Polym. Sci. Part B: Polym. Phys.* **37**, 3488 (1999).
11. E. S. Taylor, *Dimensional Analysis for Engineers*, (Clarendon Press, Oxford, 1974).
12. M. S. Wilm, M. Mann, *Int. J. Mass Spectrom.* **136**, 167 (1994).
13. J. Doshi, D. H. Reneker, *J. Electrostatics* **35**, 151 (1995).
14. J. P. Catchpole, G. Fulford, in *CRC Handbook of Chemistry and Physics*, 62nd ed., (CRC Press, Florida, 1981).